ELSEVIER

MAGNETIC RESONANCE IMAGING COMPATIBLE ROBOTIC SYSTEM FOR FULLY AUTOMATED BRACHYTHERAPY SEED PLACEMENT

MICHAEL MUNTENER, ALEXANDRU PATRICIU, DORU PETRISOR, DUMITRU MAZILU, HERMAN BAGGA, LOUIS KAVOUSSI, KEVIN CLEARY, AND DAN STOIANOVICI

ABSTRACT

Objectives. To introduce the development of the first magnetic resonance imaging (MRI)-compatible robotic system capable of automated brachytherapy seed placement.

Methods. An MRI-compatible robotic system was conceptualized and manufactured. The entire robot was built of nonmagnetic and dielectric materials. The key technology of the system is a unique pneumatic motor that was specifically developed for this application. Various preclinical experiments were performed to test the robot for precision and imager compatibility.

Results. The robot was fully operational within all closed-bore MRI scanners. Compatibility tests in scanners of up to 7 Tesla field intensity showed no interference of the robot with the imager. Precision tests in tissue mockups yielded a mean seed placement error of 0.72 ± 0.36 mm.

Conclusions. The robotic system is fully MRI compatible. The new technology allows for automated and highly accurate operation within MRI scanners and does not deteriorate the MRI quality. We believe that this robot may become a useful instrument for image-guided prostate interventions. UROLOGY **68:** 1313–1317, 2006. © 2006 Elsevier Inc.

Permanent prostate brachytherapy (PPB) is one of the most frequently chosen treatment options for patients with clinically localized prostate cancer. PPB owes its low intervention-related morbidity to a rapid dose falloff effect, which allows for the delivery of high doses of radioactivity to cancerous tissue while sparing healthy adjacent structures. The radioactive seeds are usually implanted under transrectal ultrasound guidance according to a previously developed treatment plan.

The success of image-guided interventions (IGIs) such as PPB depends on the quality of the image used for the visualization of the target, as well as on the ability to deploy the procedure needle/probe accurately to the desired target. Magnetic resonance imaging (MRI) provides the best visualization of the prostate and its surrounding anatomy,[1] which should make it the image modality of choice to guide brachytherapy seed placement. In addition, MRI can be used to make intraoperative adjustments to the dosimetry plan, permitting the deployment of additional radioactive sources in accidentally underdosed areas.[2] The principal limitation to its routine use in PPB, and IGIs in general, is the complex and challenging environment[3] inherent to MRI technology and the constrained ergonomics of closed-bore scanners. To date, only a limited number of centers have reported their experience with MRI-guided prostatic interventions.[4–7]

In the standard PPB procedure, manual needle insertion is guided by a template that is secured to the perineum. In general, this is an effective means with which to achieve the desired seed distribution; however, seed placement error is a well-recognized problem.[8–11] As a result, a loss of dosi-

This work was supported in part by the Prostate Cancer Foundation and the National Institutes of Health (CA088232). The contents are solely the responsibility of the authors and do not necessarily represent the official views of the PCF or the NIH.

From the URobotics Laboratory, Department of Urology, Johns Hopkins Medical Institutions, Baltimore, Maryland; Department of Urology, North Shore Long Island Jewish Health System, Long Island, New York; Department of Radiology, Georgetown University Medical Center, Washington, DC

Reprint requests: Michael Muntener, M.D., James Buchanan Brady Urological Institute, Johns Hopkins Hospital, 600 North Wolfe Street, Marburg 1, Baltimore, MD 21287-2101. E-mail: muntener@jhmi.edu

Submitted: March 2, 2006, accepted (with revisions): August 22, 2006

0090-4295/06/$32.00
doi:10.1016/j.urology.2006.08.1089

metric coverage from treatment plan to postimplant dosimetry has been reported.[12] However, postimplant dosimetry is one of the best predictors of treatment success[13] and has been found to be correlated with the quality of life of patients who have undergone PPB.[14] Seed placement precision has also been recognized as the limiting factor for the improvement of dose distribution.[15]

Robots are known to be accurate manipulation devices that can share the digital workspace of MR imagers. It is, therefore, conceivable that an MRI-guided robot could improve the accuracy of brachytherapy seed placement. However, most of the components currently used in robots, particularly their electromagnetic motors, are by principle incompatible with the MRI environment.

We designed and developed a fully MRI-compatible robotic system designed to interact with the patient in a closed-bore MRI scanner and to deploy brachytherapy seeds under MRI guidance. We report on the preclinical tests designed to assess the MRI compatibility of this robot, as well as its precision in placing brachytherapy seeds in tissue mockups.

A demonstration of the robotic system in action is provided in the supplementary video presentation (Video 1).

MATERIAL AND METHODS

Robotic System

The system consists of two major components. The first is the controller unit, which includes a computer, motion-control elements, and a series of electropneumatic and electro-optical interfaces. These controller elements are located outside the imager's room and are connected to the robot with several hoses. The second component of the system is the robot itself, which fits into the 50-cm bore of a standard closed MRI scanner and is designed to interact with the patient within the imager.

The robot has five degrees-of-freedom (DOFs) to place and orient an end-effector as desired. The end-effector has an additional DOF to set the depth of needle insertion and three DOFs to manipulate a titanium needle and to deploy brachytherapy seeds automatically. At the moment, this is the only end-effector that has been developed. However, it is easily detachable from the robot and could be replaced with other end-effectors, allowing the system to engage in different automated IGIs, such as biopsy, serum injections, or ablation procedures. To achieve full MRI compatibility, the entire robot is built of nonmagnetic and dielectric materials, including ceramic, plastic, and rubber materials. The only exception is the MRI-compatible titanium needle.

The completely novel concept, however, is that the robot does not use any electricity whatsoever. A new type of pneumatic actuator was specifically developed for this application. Unlike other types of pneumatic motors, this new motor (PneuStep[16]) achieves high precision of motion in a safe and easily controllable manner using a stepping motor principle. The linear size of one step is 0.055 mm. Pressure waves are used to set the motor in motion. These waves are created by a pneumatic distributor remotely located in the controller unit and are transmitted to the robot through air hoses. The actuation is encoded by fiber optics so that the motors use pressure and light but no electricity. These features prevent the robot from creating any interference with the electromagnetic environment inherent to MRI technology.

To provide the safety standard required for use in medical applications, the robot's motors are built for fail-safe operation. Any form of malfunction leads to a lock and cannot result in uncontrolled motion beyond the size of one step (0.055 mm).

Fiducial markers attached to the end-effector are used to register the robot in the MRI scanner (Fig. 1). Once the robot is fixed within the scanner, its position can be determined by obtaining volumetric MR images of the markers. Registration

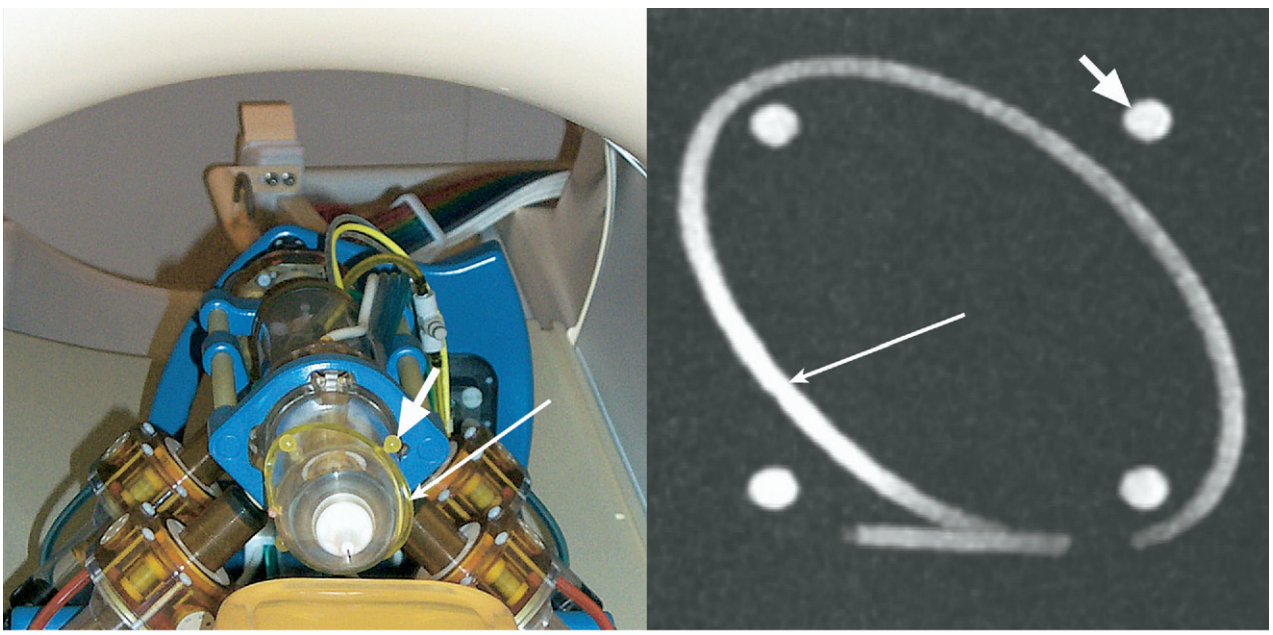

A B

FIGURE 1. *Four balls (short arrows) and one tube (long arrows) are used for registration of robot in MRI. (A) Test setup of robot in MRI scanner. (B) Three-dimensional reconstruction of MRI of markers.*

of the robot and calibration between its coordinate system and the coordinate system of the MRI scanner is then provided by custom software.

MRI Compatibility Tests

To determine its MRI compatibility, the robot was operated and imaged in three MRI scanners with field strengths of 0.5, 1.5, and 3.0 Tesla (T). Additionally, it was precision tested in a 7T research MRI scanner (see below). Because the 100-mm bore of that research MRI scanner could not accommodate the whole robot, the end-effector alone was operated within the high-field-strength scanner.

Motion Accuracy Tests

The initial tests were performed to assess the basic motion capabilities of the robot. In the motion tests, the robot was commanded to sequentially position in eight extreme points of the work space. Each cycle was then repeated 20 times. An optical tracking system (Polaris, NDI, Waterloo, Ontario, Canada) was used to measure the actual position of the robot with an active six DOFs marker mounted on the frame of the end-effector. To reduce measurement errors, each position was averaged for 10 data acquisitions with the robot at rest. A similar motion repeatability experiment was performed with the robot positioned within a closed-bore 1.5T MRI scanner to determine whether the precision of the robot's motion would be influenced by the magnetic field.

In additional tests, the accuracy of the seed placement was determined in tissue mockups made of Farmer Summer Sausage (Fred Usinger, Milwaukee, Wis) embedded in a clear gel. We chose this sausage for its relatively tough skin, firm consistency, and inhomogeneous content. The computer was programmed with the x, y, and z coordinates of the planned seed positions. The deployment of the nonradioactive stainless steel seeds was then performed by the robot in a fully automated fashion. Next, a computed tomography scan (slice thickness 0.75 mm, interslice spacing 0 mm) of the tissue mockup was acquired. On this three-dimensional (3D) computed tomography volume, the seeds were identified, and each seed's relative position with respect to its preplanned position was measured along all three axes using custom-developed software. The norm of the error vector (measuring the distance between the deployed and desired 3D location of a seed) was recorded for every seed. The accuracy of seed placement was measured in a total of 125 seeds.

Finally, a motion accuracy test was conducted within a 7T research MRI scanner (see above). In this test setup, a multimodality fiducial marker (IZI Medical Products, Baltimore, Md) was attached to the needle tip of the brachytherapy end-effector. A full 3D MRI volume was obtained (slice thickness 0.35 mm, interslice spacing 0 mm), and the robot was then programmed to move the needle over a certain distance. With the MRI marker in the new position, a full 3D MRI volume was again obtained. The actual distance the needle traveled was computed using image-to-image registration. This process was repeated 30 times.

RESULTS

MRI Compatibility

In the confined space and the electromagnetic environment of the clinical MRI scanners, no restraint of the robot's action was noted. More importantly, the presence of the robot in the scanner neither caused any interference with the MRI nor deteriorated the quality of the obtained images. Apart from the markers attached to the end-effector, the robot was invisible for the MRI. The same observation was made when the brachytherapy end-effector was operated and imaged in the 7T research MRI scanner, within which the pneumatic motor positioned the needle with the same high precision that it did outside the MRI scanner (see below). Again, no interference with the MRI scanner was noted, and visualization of the multimodality fiducial marker was equally good with or without the presence of the robot within the scanner, as well as with it at rest or in motion.

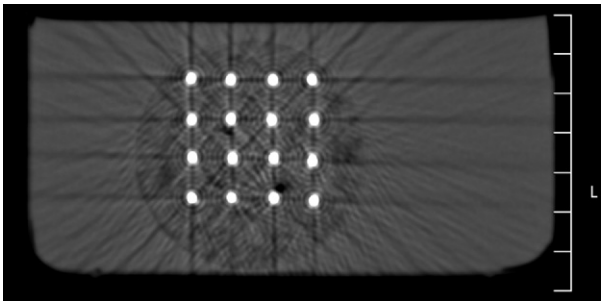

FIGURE 3. *Computed tomography scan showing 16 stainless steel seeds implanted in tissue mockup.*

Motion Accuracy

In the basic motion capability tests, the mean value of the error's norm for all experiments was 0.076 ± 0.035 mm. However, after a warm-up phase of several cycles, the errors were consistently about 0.050 mm. The respective tests in the 1.5T MRI scanner yielded a mean error value of 0.060 ± 0.032 mm. These somewhat better results recorded in the MRI scanner resulted from several unrecorded warm-up cycles performed while adjusting the robot within the confined space of the scanner.

In the tissue mockup tests, the mean placement error of the 125 stainless steel seeds was 0.72 ± 0.36 mm. A histogram of the placement error distribution is shown in Figure 2. Figure 3 shows a

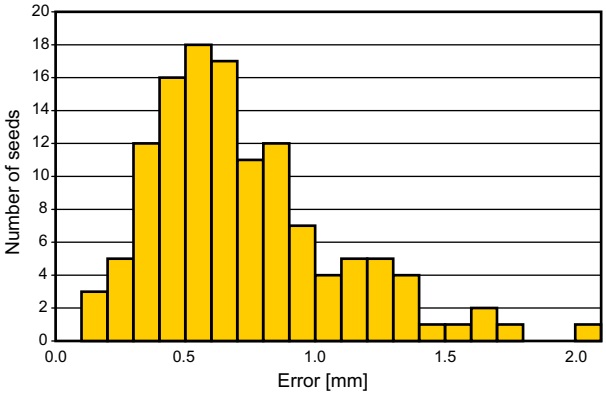

FIGURE 2. *Histogram showing placement error distribution of stainless steel seeds implanted in tissue mockups by robot.*

computed tomography scan of one of the tissue mockups with implanted stainless steel seeds.

In the 7T MRI scanner, the end-effector moved the brachytherapy needle with a mean placement error of 0.047 ± 0.053 mm.

COMMENT

Modern medicine relies heavily on technical equipment, and current technology is evolving very rapidly. This progress allows for existing diagnostic and therapeutic interventions to become more efficient and also helps in the development of new treatment modalities. Because of its relatively fixed position and its good perineal and transrectal accessibility, the prostate is an optimal target for image-guided interventions. As such, ultrasound-guided prostate biopsy and PPB are common procedures in modern urologic practice. The advantages of ultrasonography are its widespread availability and easy-to-use technology, as well as its real-time imaging. However, MRI is superior to ultrasonography with regard to visualization of the prostate and the surrounding anatomy.[1] Additionally, advances in MRI technology, such as MR spectroscopic imaging, dynamic contrast-enhanced MRI, and the availability of greater field strength scanners, make MRI an increasingly attractive imaging modality for targeting prostate cancer.[17–19]

PPB is a procedure that potentially benefits from MRI guidance. In addition to the excellent visualization of the prostate, intraoperative MRI can provide dosimetric feedback. This can allow significant aberrations from the preplanned dosimetric coverage to be detected during the procedure, with the opportunity to deploy additional radioactive seeds into underdosed areas.[10] In contrast, transrectal ultrasonography does not provide reliable seed localization and attempts to obtain intraoperative dosimetric information require co-registration and fusion with another imaging modality.[20,21] This process makes the procedure complicated and subject to registration errors. Therefore, intraoperative dosimetric feedback is not commonly used in PPB.

Ideally, MRI guidance would be combined with the precision of robotic manipulation. Robots are capable of working more accurately than humans and, as digital devices, can be easily programmed to navigate in a 3D coordinate system. In the case of PPB, this means that a robot could very accurately place all its planned seeds through one or two tiny perineal skin incisions without the need for a template,[22] which constrains the possible trajectories of the needle and, in some cases, may even leave parts of the prostate inaccessible for seed placement.[23] Improvements in the placement of the radioactive sources are likely to translate into better cancer control, as well as reduced irradiation of healthy tissue.[13,14]

The limited accessibility of the patient within the MRI scanner and the incompatibility of most components commonly used in robotics, however, have made the development of an MRI-guided robot a very difficult engineering task.

To date, few centers have reported their experience with MRI-guided prostatic interventions. Investigators from Harvard University were the first to perform MRI-guided PPB and prostate biopsy.[2,5,24] They used a transperineal approach in an open, low-field strength (0.5T) MRI scanner and correlated the interventional MRI with images previously acquired in a 1.5T scanner. Very recently, investigators from the same group reported on a robotic manipulator designed to position a guide for MRI-controlled manual needle insertion.[25] Other groups have reported on transperineal and transrectal MRI-guided prostate interventions within high-field strength, closed-bore scanners.[4,26,27] These investigators have used custom-built MRI-compatible needle guides or templates to assist the physician in the placement of the needles.

The device we have introduced represents the first fully MRI-compatible robot. The key technology of the system is the unique pneumatic stepper motor,[16] which is completely compatible with the electromagnetic environment of the MRI and allows for very precise actuation within the imager. Previous research in this field has commonly relied on piezoelectric motors.[28–30] These are magnetism free but use high-frequency currents, creating image distortion if operated closer than 0.5 m from the MRI isocenter.[29] Our experiments have shown that our robot does not interfere with MRI when it is operated within the magnet. Moreover, the compact design of the device deals with one of the best-known difficulties of interventional MRI—patient accessibility. By fitting into a standard 50-cm bore, along with the patient, our robot allows for interaction with the patient inside the scanner. This obviates the necessity of moving the patient in and out of a closed scanner for imaging and manual needle insertion, respectively.

Under ex vivo conditions, the results of our precision tests compared favorably with the accuracy that has been reported in other MRI-guided prostatic interventions.[10,27] By using on-line MRI guidance, it is conceivable that a device such as our robotic system could improve the accuracy of seed placement in PPB and permit a more customized and targeted distribution of the radioactive sources. As a next step, however, our results need to be corroborated in additional experiments including MRI registration and animal trials.

Because of the modular structure of the robot, it will be easy in the future to exchange the brachy-

therapy end-effector with one designed for a different procedure. Alternative end-effectors could be designed to take biopsies, inject liquid agents, and insert cryotherapy or radiofrequency probes. In this way, the robot could potentially improve the performance of other IGIs and could also play an important role in the validation and application of new targeted procedures emerging for the diagnosis and therapy of prostatic disease.

CONCLUSIONS

We have presented the first fully MRI-compatible robotic system. In the present configuration, it is capable of automated and highly accurate brachytherapy seed placement within a closed-bore scanner and does not deteriorate the quality of MRI. Before any clinical use, more extensive testing is necessary. We believe that because of its promising technology, this robot may become a useful instrument for image-guided prostate interventions.

REFERENCES

1. Yu KK, and Hricak H: Imaging prostate cancer. Radiol Clin North Am **38:** 59–85, 2000.
2. D'Amico AV, Cormack RA, and Tempany CM: MRI-guided diagnosis and treatment of prostate cancer. N Engl J Med **344:** 776–777, 2001.
3. Atalar E, and Menard C: MR-guided interventions for prostate cancer. Magn Reson Imaging Clin North Am **13:** 491–504, 2005.
4. Beyersdorff D, Winkel A, Hamm B, *et al:* MR imaging-guided prostate biopsy with a closed MR unit at 1.5 T: initial results. Radiology **234:** 576–581, 2005.
5. D'Amico AV, Cormack R, Tempany CM, *et al:* Real-time magnetic resonance image-guided interstitial brachytherapy in the treatment of select patients with clinically localized prostate cancer. Int J Radiat Oncol Biol Phys **42:** 507–515, 1998.
6. Kaplan I, Oldenburg NE, Meskell P, *et al:* Real time MRI-ultrasound image guided stereotactic prostate biopsy. Magn Reson Imaging **20:** 295–299, 2002.
7. Susil RC, Krieger A, Derbyshire JA, *et al:* System for MR image-guided prostate interventions: canine study. Radiology **228:** 886–894, 2003.
8. Ankem MK, DeCarvalho VS, Harangozo AM, *et al:* Implications of radioactive seed migration to the lungs after prostate brachytherapy. Urology **59:** 555–559, 2002.
9. Beaulieu L, Archambault L, Aubin S, *et al:* The robustness of dose distributions to displacement and migration of ^{125}I permanent seed implants over a wide range of seed number, activity, and designs. Int J Radiat Oncol Biol Phys **58:** 1298–1308, 2004.
10. Cormack RA, Tempany CM, and D'Amico AV: Optimizing target coverage by dosimetric feedback during prostate brachytherapy. Int J Radiat Oncol Biol Phys **48:** 1245–1249, 2000.
11. Stock RG, Stone NN, Lo YC, *et al:* Postimplant dosimetry for (125)I prostate implants: definitions and factors affecting outcome. Int J Radiat Oncol Biol Phys **48:** 899–906, 2000.
12. Bice WS Jr, Prestidge BR, Grimm PD, *et al:* Centralized multiinstitutional postimplant analysis for interstitial prostate brachytherapy. Int J Radiat Oncol Biol Phys **41:** 921–927, 1998.
13. Potters L, Morgenstern C, Calugaru E, *et al:* 12-Year outcomes following permanent prostate brachytherapy in patients with clinically localized prostate cancer. J Urol **173:** 1562–1566, 2005.
14. Van Gellekom MP, Moerland MA, Van Vulpen M, *et al:* Quality of life of patients after permanent prostate brachytherapy in relation to dosimetry. Int J Radiat Oncol Biol Phys **63:** 772–780, 2005.
15. Roberson PL, Narayana V, McShan DL, *et al:* Source placement error for permanent implant of the prostate. Med Phys **24:** 251–257, 1997.
16. Stoianovici D, Patriciu A, Mazilu D, *et al:* A new type of motor: pneumatic step motor. IEEE/ASME Transact Mechatron (in press).
17. Kurhanewicz J, Swanson MG, Nelson SJ, *et al:* Combined magnetic resonance imaging and spectroscopic imaging approach to molecular imaging of prostate cancer. J Magn Reson Imaging **16:** 451–463, 2002.
18. Menard C, Susil RC, Choyke P, *et al:* An interventional magnetic resonance imaging technique for the molecular characterization of intraprostatic dynamic contrast enhancement. Mol Imaging **4:** 63–66, 2005.
19. Rajesh A, and Coakley FV: MR imaging and MR spectroscopic imaging of prostate cancer. Magn Reson Imaging Clin North Am **12:** 557–579, 2004.
20. Han BH, Wallner K, Merrick G, *et al:* Prostate brachytherapy seed identification on post-implant TRUS images. Med Phys **30:** 898–900, 2003.
21. Gong L, Cho PS, Han BH, *et al:* Ultrasonography and fluoroscopic fusion for prostate brachytherapy dosimetry. Int J Radiat Oncol Biol Phys **54:** 1322–1330, 2002.
22. Van Gellekom MP, Moerland MA, Battermann JJ, *et al:* MRI-guided prostate brachytherapy with single needle method—a planning study. Radiother Oncol **71:** 327–332, 2004.
23. Nag S, Beyer D, Friedland J, *et al:* American Brachytherapy Society (ABS) recommendations for transperineal permanent brachytherapy of prostate cancer. Int J Radiat Oncol Biol Phys **44:** 789–799, 1999.
24. D'Amico AV, Tempany CM, Cormack R, *et al:* Transperineal magnetic resonance image guided prostate biopsy. J Urol **164:** 385–387, 2000.
25. Dimaio SP, Pieper S, Chinzei K, *et al:* Robot-assisted needle placement in open-MRI: system architecture, integration and validation. Stud Health Technol Inform **119:** 126–131, 2005.
26. Menard C, Susil RC, Choyke P, *et al:* MRI-guided HDR prostate brachytherapy in standard 1.5T scanner. Int J Radiat Oncol Biol Phys **59:** 1414–1423, 2004.
27. Susil RC, Menard C, Krieger A, *et al:* Transrectal prostate biopsy and fiducial marker placement in a standard 1.5T magnetic resonance imaging scanner. J Urol **175:** 113–120, 2006.
28. Chinzei K, and Miller K: Towards MRI guided surgical manipulator. Med Sci Monit **7:** 153–163, 2001.
29. Hempel E, Fischer H, Gumb L, *et al:* An MRI-compatible surgical robot for precise radiological interventions. Comput Aided Surg **8:** 180–191, 2003.
30. Tsekos NV, Ozcan A, and Christoforou E: A prototype manipulator for magnetic resonance-guided interventions inside standard cylindrical magnetic resonance imaging scanners. J Biomech Eng **127:** 972–980, 2005.

Video Clips cited in this article can be found on the internet at: http://www.goldjournal.net